This poster participates in OSP
Outstanding Student Poster Contest

NICHOLAS SCHOOL OF THE ENVIRONMENT AND EARTH SCIENCES DUKE UNIVERSITY

DAAD Deutscher Akademischer Austausch Dienst German Academic Exchange Service

Reconciling tracer and float observations of the export pathways of Labrador Sea Water

Stefan. F. Gary[1]*, M. Susan. Lozier[1], Arne Biastoch[2] and Claus. W. Böning[2]
* stefan.gary@duke.edu
[1]Duke University, [2]IFM-GEOMAR Leibniz-Institut für Meereswissenschaften

EGU2011-8851
OS1.1
XY527

(1) Motivation: Are Lagrangian and Eulerian observations consistent with each other?

For more than 50 years, it has been hypothesized that the Deep Western Boundary Current (DWBC) is the continuous, primary conduit of Labrador Sea Water (LSW) exported from the high-latitude North Atlantic to the equator. Observations that contribute to this hypothesis are that the waters of the DWBC have greater equatorward velocities, higher concentrations of passive tracers, and are younger compared to the ocean interior. However, most of the floats launched in the DWBC in the Labrador Sea are quickly ejected from the DWBC and follow an interior pathway to the subtropics.

QUESTION: How can there be a high-concentration core of passive tracers in the DWBC while most floats that are launched in the DWBC are ejected comparatively quickly?

HYPOTHESIS: Tracer observations are compatible with the existence of both DWBC and basin-interior export pathways.

(2) Background: What are the LSW pathways?

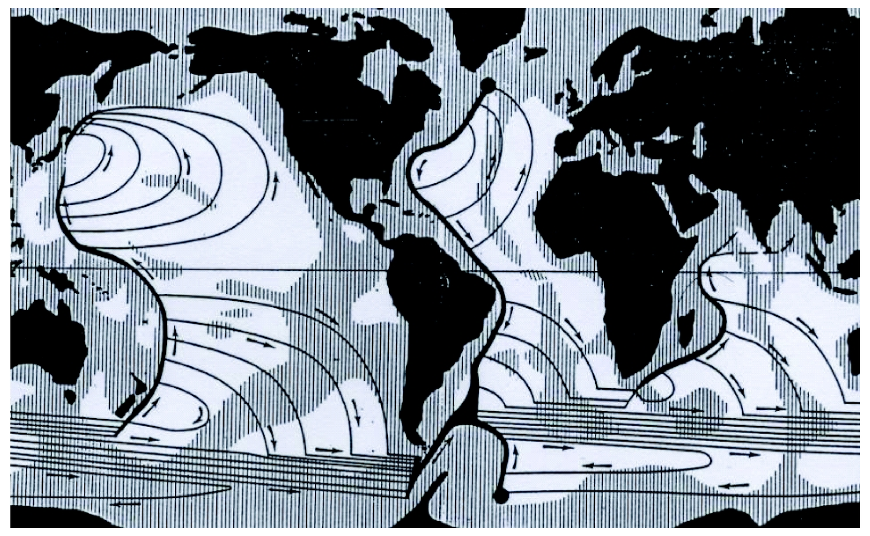

Figure 1 | The Stommel-Arons vorticity balance is

$$\beta v = f\frac{\partial w}{\partial z}$$

where f is the Coriolis parameter, $\beta = \partial f/\partial y$, v is the meridional velocity, and w is the vertical velocity[7]. Flow in the interior is hypothesized to be poleward due to a distributed upwelling from the abyssal layer into the upper layer. This upwelling is proposed as a mechanism to compensate for deep convection at high latitudes. In this model, the DWBC is the return limb of the interior poleward flow.

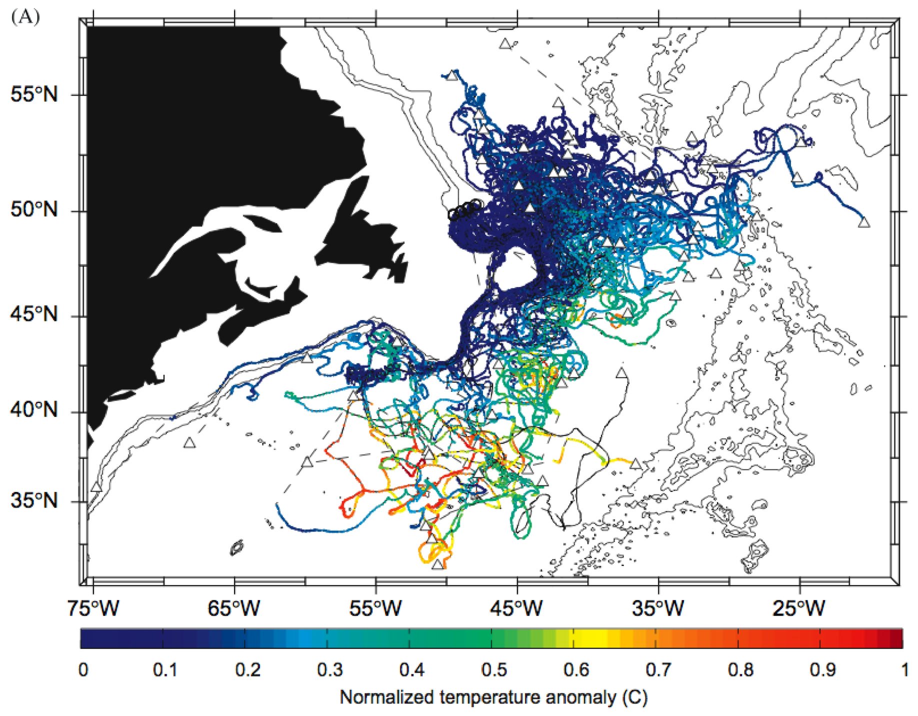

Figure 2 | Bower et al. (2011) show that although some floats launched at 700 and 1500 m in the DWBC remain in the DWBC, the majority of the floats follow interior pathways.

There is observational evidence for equatorward interior pathways of LSW. This seems to contradict the first order vorticity balance.

(3) Data sources, methods, and model

(1) A hydrographic climatology was constructed for the North Atlantic using historical to 2009 CTD and bottle data from the National Ocean Data Center (NODC). The data were quality-controlled with a statistical check in isopycnal coordinates using the HydroBase2 package[5].
(2) CFC-11 observations were taken from CARINA 1.0[6,8], TTO-NAS[4], Line W[9], & NODC.
(3) We use output from the ORCA025 model[1], a 1/4° resolution, z-level coordinate, global configuration of the NEMO 2.3 ocean general circulation model. Velocity fields are available as 5-day averages and the CFC-11 fields (computed online) are available as monthly averages.
(4) Trajectories were computed offline from the 1980-2004 ORCA025 velocity fields with the ARIANE package[3].

(4) Tracer signal in the boundary & interior

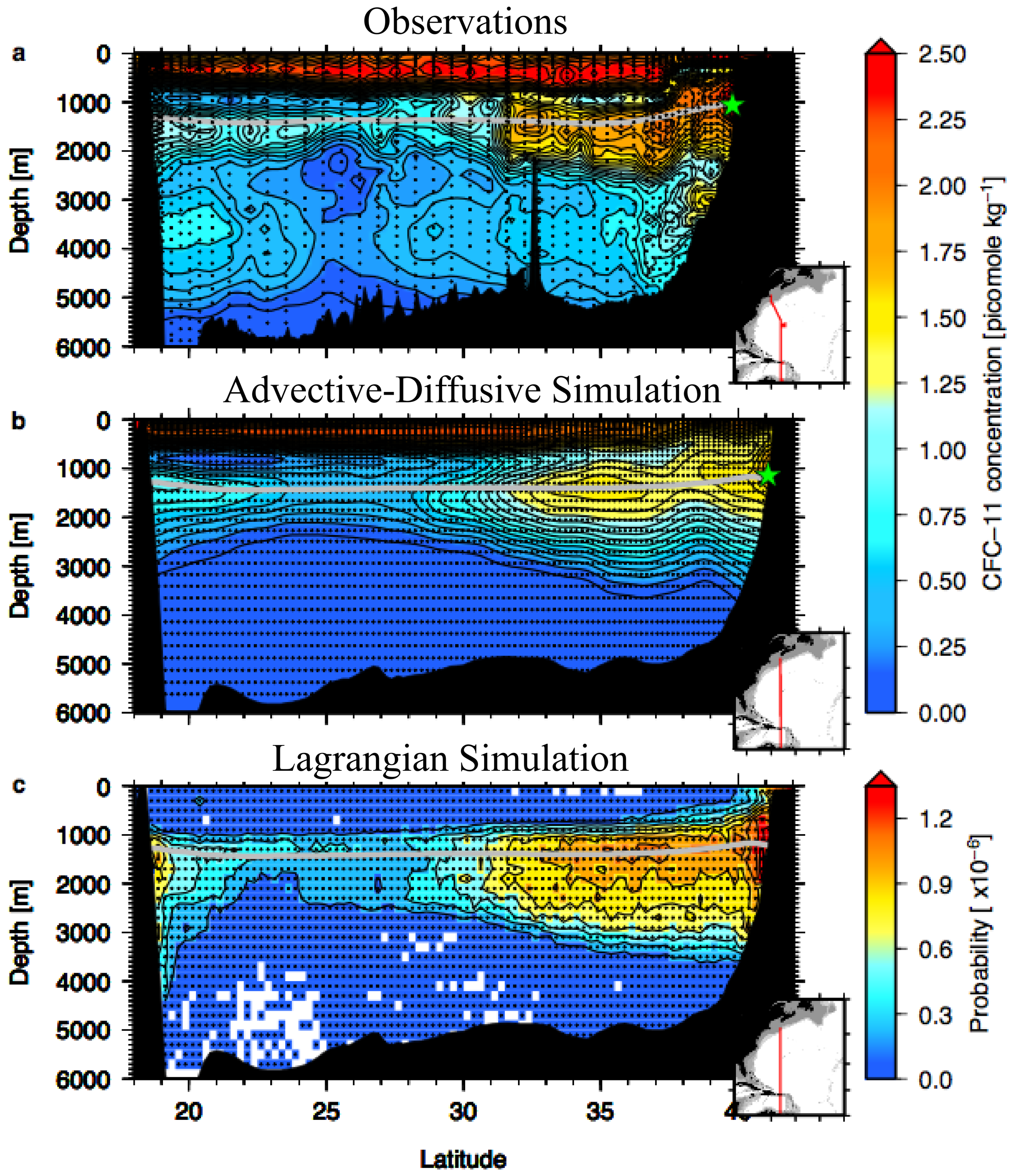

Figure 3 | **a,** CFC-11 from R/V Knorr cruise 316 (10/24/03 to 11/12/03, WOD US017320).

b, Mean November 2003 CFC-11 from ORCA025. Green stars are the instantaneous location of the highest CFC-11 concentration below 500 m depth and inshore of the 4000 m isobath, an estimate of the offshore edge of the DWBC.

c, Section of Lagrangian particle position probability volume computed from 609,055 floats launched at the surface of the ORCA025 Labrador Sea. Monthly particle positions over a 50 year simulation were used to construct the probability a float is in each ¼° x ¼° x 200 m bin.

There are significant amounts of tracer in the basin interior as well as high concentrations in the DWBC. The DWBC tracer core and basin interior tracer signals are reproduced in an advective-diffusive simulation of tracer and the purely advective spreading of simulated particles in ORCA025.

(5) Propagation of tracer signal

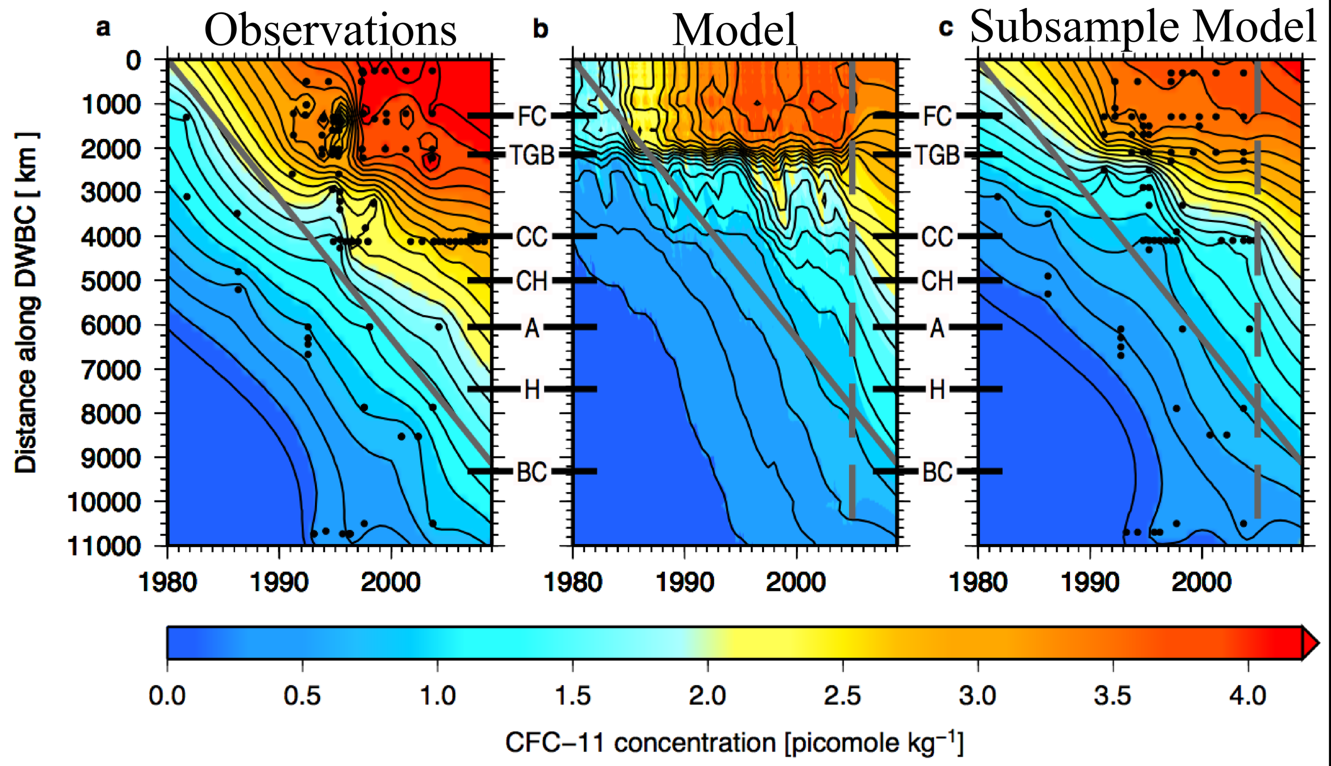

Figure 4 | **a,** DWBC CFC-11 core observations. Contoured shading is interpolated between observations (black dots) onto a 200 km x 6 month grid. Each dot is the CFC-11 maximum below 500 m and inshore of 4000 m; one dot is the green star in Fig. 3a. **b,** DWBC CFC-11 core in ORCA025 tracer fields. Contour lines are a smoothed (200 km x 6 months) version of the background shaded map (¼° x 5 days). **c,** DWBC CFC-11 core in ORCA025 subsampled at the approximate time and place of each dot in panel a. Distance along the DWBC is 0 km at 55°N in the Labrador Sea and passes FC (Flemish Cap), TGB (Tail of the Grand Banks), CC (Cape Cod), CH (Cape Hatteras), A (Abaco), H (Haiti), and BC (Brazil Coast). The solid gray line is 1 cm s^{-1} and the dashed gray line is the end of the model run.

The DWBC tracer core signal moves equatorward at ~1 cm/s, less than the ~20 cm/s speed of the DWBC. The signal appears continuous but sampling could mask a discontinuity at the Subpolar-Subtropical Gyre boundary.

(6) Mean and variability of pathway transit times

ANSWER: The DWBC has the youngest waters but the largest age variability.

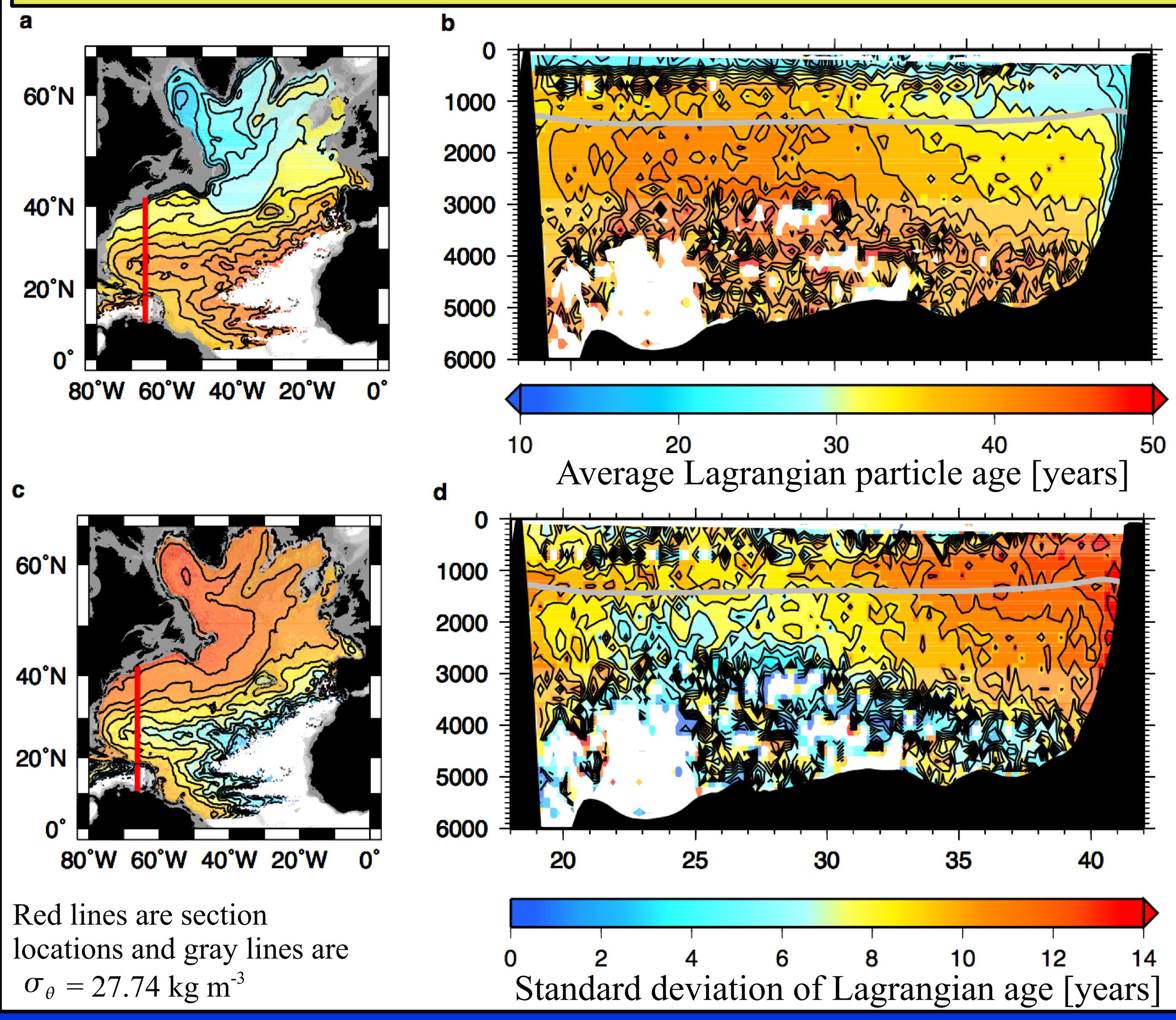

Red lines are section locations and gray lines are $\sigma_\theta = 27.74$ kg m^{-3}

Figure 5 | **a,** Average Lagrangian age of particles launched at the surface of the ORCA025 Labrador Sea that reach each ¼° x ¼° x 200 m bin at 1500 m depth after 50 years. The trajectory ensemble used to create this figure is the same as for Fig. 3c.

b, Section of the average Lagrangian age volume at 66°W.

c & d, Standard deviation of Lagrangian age in each bin shown in panels a & b.

(7) Vorticity balance at depth

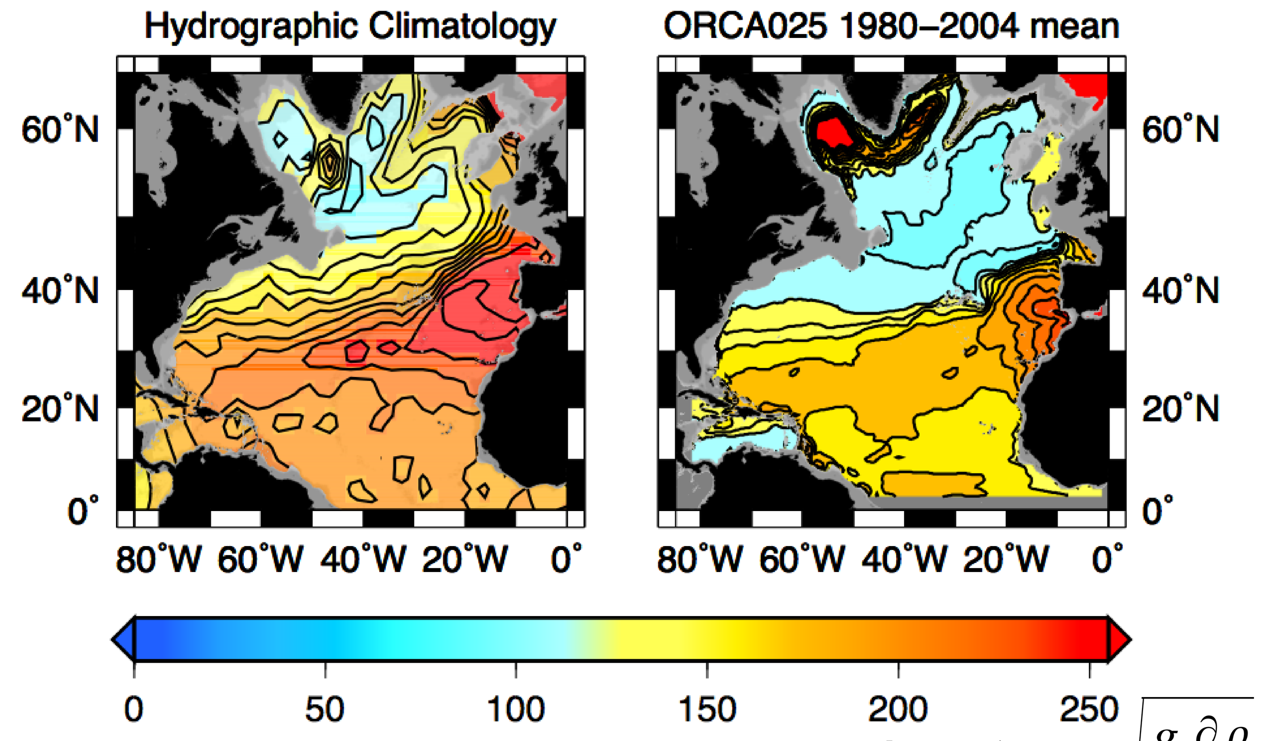

Figure 6 | Isopycnal buoyancy frequency, N [x10^{-5} rad s^{-1}], $N = \sqrt{\frac{g}{\rho}\frac{\partial \rho}{\partial z}}$ on $\sigma_\theta = 27.74$ kg m^{-3}. Larger N indicates thinner layers.

An LSW-level isopycnal thins southward, consistent with equatorward interior flow & the Stommel-Arons balance.

(1) Barnier, B. et al., *Ocean Dynamics*, 56, 543-567, 2006.
(2) Bower, A. et al., *Deep Sea Research II*, in press, doi:10.1016/j.dsr2.2010.10.060, 2011.
(3) Blanke, B. & Grima, N., ARIANE v2.2.6, http://stockage.univ-brest.fr/~grima/Ariane/
(4) Bullister, J., personal communication, 2010.
(5) Curry, R. G. Hydrobase2, http://www.whoi.edu/science/PO/hydrobase/
(6) Steinfeldt, R. et al., *Earth System Science Data*, 2, 1-15, 2010.
(7) Stommel, H., *Deep-Sea Res.*, 5(1), 80-82, 1958.
(8) Tanhua, T. et al., doi:10.3334/CDIAC/otg.ndp091, 2008.
(9) Toole, J. et al., http://www.whoi.edu/science/PO/linew/dat/index.htm

The authors gratefully acknowledge the support of the NSF and the DAAD